Original Article

Identification of the miRNAome in human fracture callus and nonunion tissues

Michael Hadjiargyrou [a,*], Leonidas Salichos [a], Peter Kloen [b,c]

[a] *Department of Biological & Chemical Sciences, New York Institute of Technology, Old Westbury, NY, 11568, USA*
[b] *Department of Orthopedic Surgery and Sports Medicine, Amsterdam UMC Location Meibergdreef, Amsterdam, the Netherlands*
[c] *Amsterdam Movement Sciences, (Tissue Function and Regeneration), Amsterdam, the Netherlands*

ARTICLE INFO

ABSTRACT

Background: Nonunions remain a challenging post-traumatic complication that often leads to a financial and health burden that affects the patient's quality of life. Despite a wealth of knowledge about fracture repair, especially gene and more recently miRNA expression, much remains unknown about the molecular differences between normal physiological repair (callus tissue) and a nonunion. To probe this lack of knowledge, we embarked on a study that sought to identify and compare the human miRNAome of normal bone to that present in a normal fracture callus and those from two different classic nonunion types, hypertrophic and oligotrophic.

Methods: Normal bone and callus tissue samples were harvested during revision surgery from patients with physiological fracture repair and nonunions (hypertrophic and oligotrophic) and analyzed using histology. Also, miRNAs were isolated and screened using microarrays followed by bioinformatic analyses, including, differential expression, pathways and biological processes, as well as elucidation of target genes.

Results: Out of 30,424 mature miRNAs (from 203 organisms) screened via microarrays, 635 (~2.1%) miRNAs were found to be upregulated and 855 (~2.8%) downregulated in the fracture callus and nonunion tissues as compared to intact bone. As our tissue samples were derived from humans, we focused on the human miRNAs and out of the 4223 human miRNAs, 86 miRNAs (~2.0%) were upregulated and 51 (~1.2%) were downregulated. Although there were similarities between the three experimental samples, we also found specific miRNAs that were unique to individual samples. We further identified the predicted target genes from these differentially expressed miRNAs as well as the relevant biological processes, including specific signaling pathways that are activated in all three experimental samples.

Conclusion: Collectively, this is the first comprehensive study reporting on the miRNAome of intact bone as compared to fracture callus and nonunion tissues. Further, we identify specific miRNAs involved in normal physiological fracture repair as well as those of nonunions.

The translational potential of this article: The data generated from this study further increase our molecular understanding of the roles of miRNAs during normal and aberrant fracture repair and this knowledge can be used in the future in the development of miRNA-based therapeutics for skeletal regeneration.

1. Introduction

Fracture repair is a complex biological process that ultimately results in bone regeneration and restoration of biomechanical, biochemical, physiological and functional properties [1]. In the United States alone, 16 million people each year fracture a bone and while most heal within 6–12 weeks with (near) full recovery of function, unfortunately, for some patients, the fracture does not heal, and it becomes either a delayed or nonunion [1]. Although delayed unions can still heal without surgical intervention, a nonunion does not, and often causes prolonged pain and disability with negative effects on mental and physical health and general quality of life.

Most often, nonunions affect the tibia, scaphoid and humerus. Related factors can either be patient-derived, such as smoking, opioid use, diabetes mellitus, nutrition, age, general health and use of medication (e.g., steroids, NSAIDS, bisphosphonates). More important causes for a nonunion are fracture-associated factors such as a high-energy injury, open fracture, segmental or comminuted fracture pattern. Lastly, there

are doctor-derived factors, including poorly performed surgery (stripping of soft tissues and periosteum), poor reduction and/or poorly applied or incorrect implants. Further, nonunions are classically divided in three types according to Weber and Cech (1976) [2]: atrophic, oligotrophic and hypertrophic. This classification is based on their radiographic appearance. A hypertrophic nonunion has the appearance of an elephant's foot or a horse hoof, the oligotrophic and atrophic nonunion have a lack of callus. Further, diagnosis is also based on plain radiographs and/or CT (computed tomography) evaluation showing absence of bony bridging. In addition, a patient with a nonunion often complains of pain or instability and inability to weight-bear. Loosening or failure of hardware seen radiologically, suggests instability and failure of fixation. Once the diagnosis of a nonunion is made, there is no sense in delaying surgical intervention. The clinician treating a nonunion should strive for optimization of the mechanical environment. Once the mechanical environment is optimized surgically, the "normal" biology will often recover. The fixation should neither be too stiff or too flexible. The ideal strain rate (a measure of deformity calculated by delta length/length) is thought to be between 2 and 10% [3].

The atrophic nonunion has long been considered avascular, whereas the oligo and hypertrophic nonunion are considered more vascular and thus biologically active. Interestingly, experimental evidence has shown that biological activity persists in an atrophic nonunion [4], and that atrophic nonunions are not necessarily avascular, suggesting the original Weber and Cech classification may need to be revised. More recently, the concept of bone healing and nonunion theory (BHN) suggests it might be better to consider a nonunion as primarily mechanical or biological in origin [3]. Mechanical instability seems to dominate in clinical practice. It is rare that the biological potential is lost. Treatment for a nonunion typically involves mechanical stabilization. This is often preceded by extensile debridement with removal of failed hardware, avital tissue, followed by alignment and rigid fixation. Augmentation of the healing response is done by adding bone graft (autologous or homologous) for the atrophic and most oligotrophic nonunions. For the hypertrophic nonunion, optimizing the stability of the nonunion will generally lead to bone healing. This is achieved by compression of the nonunion ends together. There is no consensus on the use of homologous or autologous bone graft. The use of mesenchymal stem cells is still in its infancy. Biological adjuvants including growth factors such as Bone Morphogenetic Proteins (BMP) [5], demineralized bone matrix and systemic medication (parathormone (PTH), sclerostin) [6,7] have not proved to be successful as of yet. As such, if we are to truly understand the biology of nonunions and be able to devise a biologically driven approach to treating them, it is imperative that we examine some of the molecular processes that underlie the nature of a nonunion.

One such process involves microRNAs (miRNAs) which are small regulatory RNA molecules that bind to target mRNAs and either lead to their enzymatic degradation or translational repression [8,9]. Previously, we reported on the involvement of miRNAs during the early phases of mammalian physiological repair [10] and we now apply the same approach in order to understand their roles in human normal fracture callus and nonunion tissues (both hypertrophic and oligotrophic). We hypothesized that miRNAs would display differential expression in these human tissues. Thus, we performed a complete profiling of all known miRNAs in RNA samples isolated from human normal bone, physiological fracture callus and tissues from hypertrophic and oligotrophic nonunions. Herein, we describe that miRNAs are indeed differentially expressed in these human samples and we also show common, as well as unique miRNAs between the samples. Additional bioinformatics analyses show many potential target mRNAs involving various key biological processes. Taken together, these data provide the first complete miRNAome analysis during normal physiological fracture repair and nonunions in humans and hopefully, will aid in understanding some of the molecular mechanisms that guide normal and/or aberrant bone healing.

2. Materials and methods

2.1. Patients and tissue samples

All patients were treated by the third author (a fellowship trained orthopedic trauma surgeon), between June 2016 and July 2020. Consent for removal of the tissue and its storage in the tissue bank in a coded fashion for research purposes was obtained from each patient per Institutional Review Board (IRB) guidelines (W20_075 #20.103, Academic Medical Center, Amsterdam). Indications for surgery were nascent (impending) malunion, nonunion, and failure of fixation or fractures that were operated on in delayed fashion. All patients presented with complaints of pain, deformity, and decreased function of the involved extremity. No patient had evidence of an active infection as determined based on radiographic, physical, laboratory, and intraoperative findings. Tissues were obtained from the iliac crest (excess harvested bone graft that was not used and considered surgical waste and could be used as control samples) or nonunions or fracture callus (Callus). The areas where tissues were harvested from are indicated by arrows in X-rays of three representative patients (Fig. 1). After removal, the tissue was inspected and judged based on appearance and feel. In general, callus has a more "rubbery" feel than nonunion tissue. Oligotrophic nonunion (NU-OT) tissues are less dense than hypertrophic nonunion (NU-HT) tissue.

Fig. 1. Representative radiographs of callus, NU-HT and NU-OT (A) Anterior-Posterior (AP) radiograph of a right femoral shaft fracture treated with a plate in a 52-yo previously healthy male. Initial treatment consisted of external fixation for 3 days, which was then converted to a minimally invasive plate fixation. Three months later the patient underwent revision fixation (based on loose plate) and a substantial amount of callus present showing by the arrow. A small portion of callus tissue was obtained as indicated by arrow. (B) AP radiograph of *a left tibia and fibula nonunion in 62-year healthy old male. Initial fracture treatment was done 2 years prior. The nonunion was classified as a hypertrophic nonunion (NU-HT, according Weber and Cech) because of the elephant foot appearance. Tissue was obtained from the center of the nonunion as indicated by the arrow (C) AP radiograph of left tibia shaft and fibula nonunion in a 47-year old healthy female. The nonunion was classified as an oligotrophic nonunion (NU-OT, according to Weber and Cech). A small portion of nonunion tissue was obtained from the central part as indicated by arrow.*

For histology, after removal from a patient, the specimen was placed in 10% neutral buffered formalin for 24 h. Routine pathology evaluation was done as part of medical care. For RNA isolation, a second representative portion of tissue was snap frozen-immediately after removal in liquid nitrogen and stored at −80 Celsius for later use.

The exclusion criteria included malignancy, infection, corticosteroid use, pregnancy, metabolic bone disease, alcohol abuse, or the use of vitamin D, calcium, or hormones. A nonunion was defined as the absence of osseous healing at six months after the operative or nonoperative treatment of a fracture. Patient characteristics are listed in Table 1. For this study, tissue specimens were obtained during surgery from patients at the time of operative repair or revision surgery of the fracture (callus, n = 4) or nonunion (n = 8). The nonunions were classified according to the Weber and Cech into hypertrophic (n = 4) or oligotrophic (n = 4), based on their radiographic appearance on the pre-operative studies. Additionally, from 4 patients there was surplus bone graft obtained from the iliac crest that was used as the negative control. The fracture calluses and nonunion tissues served as the experimental samples. The patient age, sex, location of fracture/nonunion and time since fracture are all indicated in Table 1.

2.2. Histology

Tissue specimens were processed similarly to previous studies conducted by our laboratory [11–17], Briefly, tissue specimens were fixed in 10% neutral buffered formalin for 24 h and subsequently decalcified in 10% ethylenediamine tetra acetic acid (EDTA), pH 7.2 for 3 weeks, and then embedded in paraffin. Six micrometer sections were cut using a Leica RM 2255 microtome (Leica Microsystems, Richmond Hill, ON, Canada). Following deparaffinization and hydration, sections were stained by Goldner Trichrome using standard staining procedures. Images were capture using a Zeiss Axio microscope attached to an Infinity 3 camera (Teledyne Lumenera).

2.3. RNA isolation

RNA was extracted using the RNeasy Plus Universal Mini kit (Qiagen). About 4 mm^3 of snap-frozen callus, nonunion and ileac crest bone samples were placed in 900 µl of Qiazol Lysis Reagent (Qiagen) and were homogenized with a 4 mm steel bead for 2 cycles of 2 min each at 25 Hz on a TissueLyser II (Qiagen). The homogenized samples were pipetted into a new tube and incubated for 5 min at room temperature (RT) before adding 100 ul of gDNA Eliminator Solution and vigorously shaking for 15 s. Next, 180 µl of chloroform per sample was added, thoroughly mixing the samples for 15sec, followed by 3 min incubation at RT. The samples were then centrifuged for 15 min at 12,000 g at 4 °C. The aqueous phase was transferred into a new tube and one volume of 70% ethanol was added and immediately vortexed. The solution was then added to the spin column and centrifuged for 30 s at 8000 g at RT, repeating this step until all the sample was passed through the column. The flow-through was further processed to extract miRNAs using the miRNeasy Kit (Qiagen) and following manufacturer's instructions. The RNA concentration was then determined using an Invitrogen™ Qubit™ 4 Fluorometer and Qubit RNA IQ Assay. Each RNA sample was used in miRNA microarray analyses (conducted by Stony Brook University's Medical School Genomics Core Facility).

2.4. miRNA microarrays

Total RNA (16–130 ng) from each sample (4 samples/bone condition) was labeled using the FlashTag™ Biotin HSR RNA Labeling Kit (Applied Biosystems). The RNA was initially subject to a poly(A) tailing reaction, followed by FlashTag™ Biotin HSR ligation of a Biotin-labeled 3DNA molecule (prepared as per manufacturer's protocol). For hybridization, a hybridization master mix was made consisting of the 2X hybridization mix, 27.5% formamide, 10% DMSO, 20X hybridization controls, and a control oligo (3 nM). The hybridization mix was incubated for 5 min at 99 °C and then at 45 °C for 5 min. Then, 130 µl of the hybridization cocktail was applied to each GeneChip™ miRNA 4.0 Array (Applied Biosytems) (contains all mature miRNA sequences in miRBase Release 20). Each array was incubated at 48 °C and 60 rpm for 16–18 h. The arrays were then washed and stained in an Affymetrix FS450 Fluidics Station using the FS450_0002 protocol, as per manufacturer specifications. The arrays were finally scanned with an Affymetrix GeneChip Scanner 7G and the data analyzed using the TAC 4.0.2 software. Robust Multichip Average (RMA) was used for normalization by initially performing a background correction to correct for spatial variation within individual arrays, followed by a background-corrected intensity which was calculated for each probe with the final base-2 logarithm determined. Quantile normalization was also used to correct for variation between the arrays. Finally, probe normalization was utilized to correct for variation within probe sets.

2.5. Bioinformatic analyses

To perform our differential analysis, we installed Bioconductor packages from Bioconductor repository in R [18]. These packages include oligo, affydata, ArrayExpress, limma, Biobase, Biostrings, genefilter. Additional packages (based on dependencies) include Matrix, lattice, fdrtool, rpart. Statistical analysis was performed using R. Fracture callus and nonunion tissues (hypertrophic and oligotrophic) microarray data were compared against control (intact bone) samples to identify differentially expressed miRNAs. For each group we obtained and analyzed four replicates either as an average or individually. A miRNA was considered up- or down-regulated if the average expression signal from all 4 replicates was at least 1.5-fold greater or less than the control replicates. Then the average was obtained for each time replicate and the ratios to the average of control signals were calculated and log2 transformed. Heatmaps were generated using heatmap.2 with hierarchical clustering in gplots.

Differentially expressed human miRNAs were further analyzed using miRbase [19]; we identified the corresponding miRNA transcribed from genomic regions. The genes that were targeted by those miRNAs were identified using miRDB [20] with minimal score of 90. We further conducted gene enrichment analysis for pathways and biological processes

Table 1
Patient/facture characteristics.

Tissue type	Age/ sex	Location	Time since fracture	Co-morbidities
Normal bone (Control)	52/M	Iliac crest		None
	26/M	Iliac crest		None
	28/M	Iliac crest		None
	57/F	Iliac crest		Diabetes Type I & hypertension
Fracture Callus (Callus)	77/F	Femur	3 wk	Hypertension
	52/M	Femur	3 mo	None
	16/M	Tibia	3 wk	None
	64/F	Humerus	1 mo	Mitral valve prolapse
Hypertrophic nonunion (NU-HT)	53/M	Femur	7 mo	Hypertension/ Hyperthyroidism
	62/M	Tibia	25 mo	None
	28/M	Ulna	13 mo	ADHD
	54/F	Femur	27 mo	Rheumatoid arthritis
Oligotrophic nonunion (NU-OT)	85/F	Femur	22 mo	Psoriasis/myocardial infarction
	69/F	Humerus	18 mo	None
	81/F	Femur	7 mo	Devic's (eye) disease
	47/F	Tibia	13 mo	Aortic valve replacement

Abbreviations: wk = weeks; mo = months; M = male; F = female

using DAVID Bioinformatics Resources and the Gene Ontology Resource [21]. Pathway analysis was performed using the Kyoto Encyclopedia of Genes and Genomes (KEGG) pathways. The obtained p-values were adjusted using Bonferroni corrections.

3. Results

3.1. Histological examination of tissues

Histological (Goldner's trichrome) examination of the three tissues, fracture callus and both hypertrophic and oligotrophic nonunions are shown in Fig. 2. Specifically, in low magnification images of sections from each experimental sample, we detect mostly a nicely organized mineralized (bony) fracture callus (Fig. 2A, D), whereas in the nonunion samples, the predominant tissues present are unmineralized osteoid and fibrous tissue in NU-HT(Fig. 2B, E) and the same as well as cartilage in NU-OT (Fig. 2C, F), which makes them heterogeneous in nature. Small amount of osteoid is also present in the fracture callus sample (Fig. 2A, D) but not to the extent seen in the nonunion tissues which also showed fragmentation of the tissue (Fig, 2 B and C). Additional higher magnification images reveal greater cellular details with the presence of active osteoblasts (Fig. 2G, arrows) and those trapped in the mineralized callus. In the nonunion tissues the unmineralized osteoid can be clearly seen (Fig. 2H and I) and in the NU-OT sample, chondrocytes are prevalent in the cartilage area (Fig. 2I, arrows). Lastly, sections stained with Hematoxylin and Eosin (H & E) from all tissues used in these analyses are shown in Supplementary Fig. 1 and clearly indicate tissue heterogeneity of the nonunion samples.

3.2. miRNA expression in fracture callus and nonunion tissues

Given that our previous approach with miRNA microarrays and animal models of fracture repair was very successful in identifying miRNA expression [10], we decided to utilize the same approach to identify differentially expressed miRNAs in human fracture callus and nonunion tissues. Out of the 30,424 mature miRNAs (from 203 organisms) that were present on the microarrays, 635 (~2.1%) miRNAs were found to be up-regulated and 855 (~2.8%) down-regulated in the fracture callus and nonunion tissues (NU-HT and NU-OT) as compared to control intact bone. The expression signals of these differentially regulated miRNAs are shown in a heatmap for all (Supplementary Fig. 2B) as well as separately for the upregulated and downregulated miRNAs (Supplementary Fig. 2B). The expression levels of all miRNAs by species in each experimental sample (as compared to control) are indicated in Supplementary Table 1 (sorted alphabetically by species and values presented as log2 change against the control sample [Intact bone]). Further, the expression of the 635 and 855 up-regulated and down-regulated miRNAs, respectively is shown graphically in Supplementary Fig. 2 for the Callus and the NU-HT and NU-OT tissues (Supplementary Figs. 2C and D). Lastly, the 635 up and 855 downregulated miRNAs are listed in Supplementary Tables 2 and 3, respectively (sorted alphabetically by species and values presented as log2 change against the control sample).
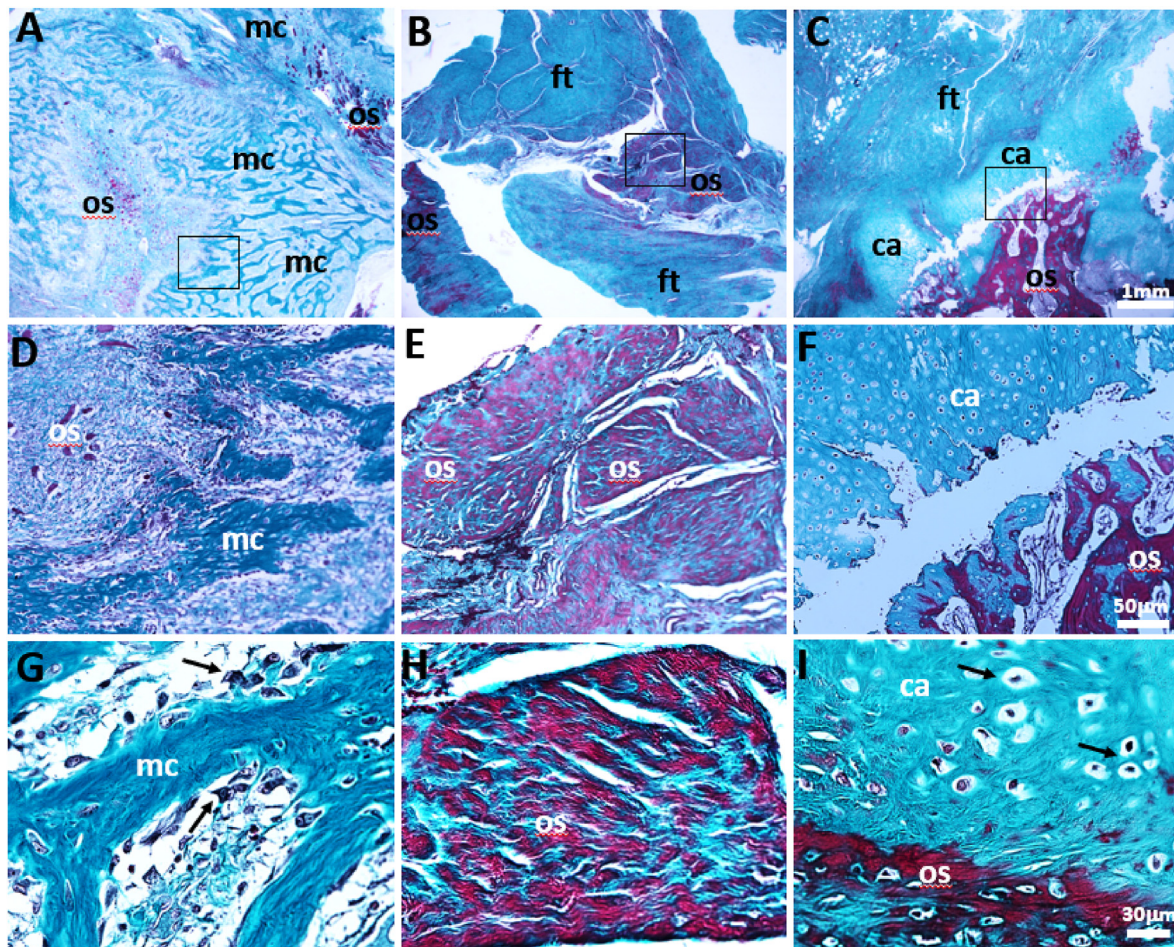

Fig. 2. Fracture callus and nonunion tissue histology. Sections of fracture callus (A, D, G) and nonunions tissues, NU-HT (B, E, H) and NU-OT (C, F, I) were stained with Goldner's trichrome. D, E, and F are enlarged images of areas shown in boxes in A, B and C, respectively. Arrows in G and I indicate osteoblasts and hypertrophic chondrocytes, respectively. mc, mineralized callus; os, osteoid, ft, fibrous tissue, ca, cartilage. Scale bar in A-C is 1 mm; D-F is 50 μm and G-I 30 μm.

As our tissue samples were derived from humans, we decided to focus on the human miRNAs for the rest of our analyses. As such, we initially looked at the total number of human miRNAs (4,223) and from those how many were differentially expressed between intact bone and the three experimental samples (fracture callus and nonunions, Supplementary Table 4). From the 4223 human miRNAs, 86 miRNAs (~2.0%) were up-regulated and 51 (~1.2%) were down-regulated in the fracture callus and nonunion tissues in comparison to control bone and listed in Supplementary Tables 5 and 6 (with values presented as log2 change against the control sample [Intact bone]), respectively. The values for each human miRNA for each of the four tissue samples used in the analyses along with the statistical analyses are shown in Supplementary Table 7. The heat maps and graphs of the upregulated and downregulated human miRNAs between the control and experimental samples are shown in Fig. 3A and C. We also show heat maps of the up and downregulated miRNAs from each of the four individual samples used for each tissue type to demonstrate the similarities/differences between them (Supplementary Figs. 3A and B).

We further examined these up- and down-regulated miRNAs (>1 log2 change) and we can observe that a subset, 15 upregulated and 12 downregulated are expressed in all 3 samples (Fig. 4A and B). Moreover, we also find some miRNAs that were present in two out of the three samples, either in callus and NU-HT or callus and NU-OT as well as just in the two nonunions samples (Fig. 4A and B). There were also up- and down-regulated miRNAs that were unique to just a single sample (Fig. 4A and B).

In addition, we examined the 20 most highly upregulated miRNAs in the three experimental samples and found that 6 are present in all three samples (Table 2). Seven of these highly expressed miRNAs were found in the top 20 between the fracture callus and NU-OT samples (Table 2). Lastly, 3 of these top 20 miRNAs, were only present between the nonunion samples (Table 2).

Fig. 4. Differential miRNA distribution in each experimental sample. A. Venn diagram indicating common upregulated miRNAs between the three experimental samples (Callus, NU-HT and NU-OT). B. Venn diagram indicating common downregulated miRNAs between the three experimental samples (Callus, NU-HT and NU-OT). Numbers in both A and B indicate the common miRNAs either between two or three samples. We also show the number of miRNAs that were exclusive to each experimental sample.

Similar analyses were conducted with the top 20 downregulated miRNAs and we found that 11 were common in the three samples (Table 3). Five were common between the fracture callus and NU-OT; one between fracture callus and NU-HT and two between the two nonunion samples (Table 3).

We also examined whether there were miRNAs that were upregulated (>0.5 log2 change), in one sample but downregulated in the other two samples by (>0.5 log2 change (using the expression data from Supplementary Tables 5 and 6). Using this approach, we identified three miRNAs that were only upregulated in the fracture callus but downregulated in both nonunion samples (Table 4). Similarly, 18 miRNAs that were
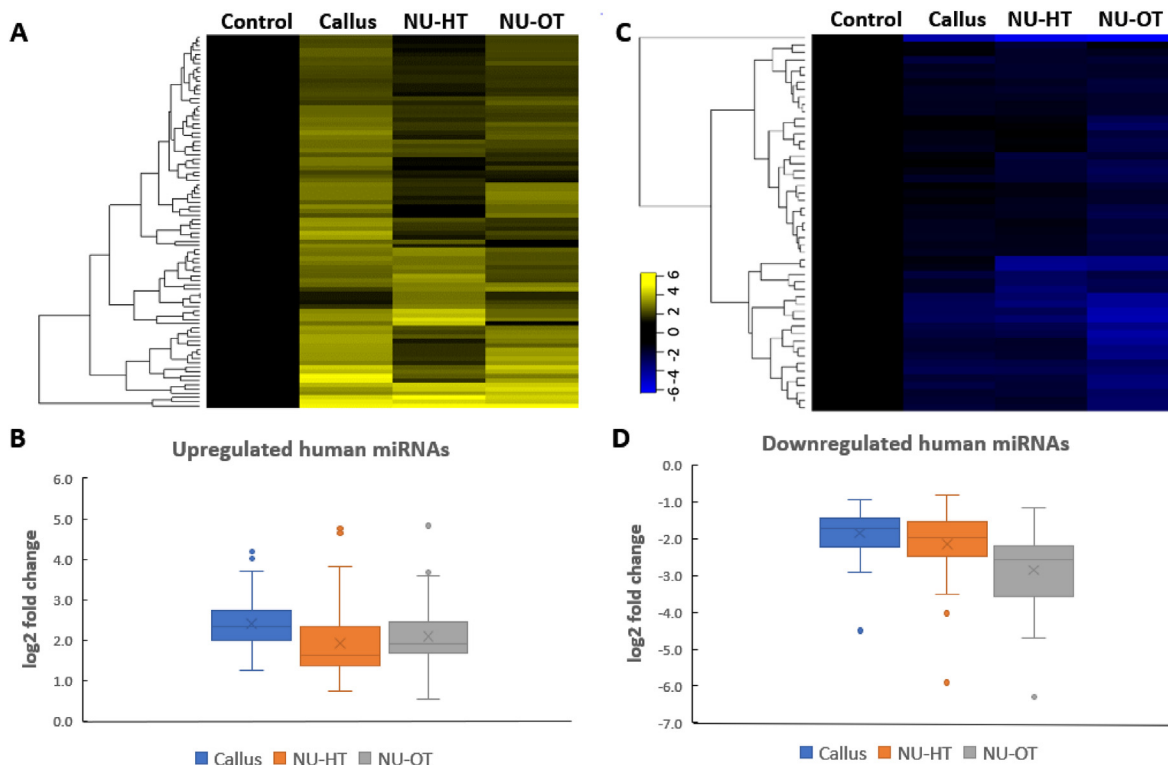

Fig. 3. Differential human miRNA expression between control (intact bone) fracture Callus and nonunion tissues (NU-HT and NU-OT). A and C. Heatmaps of the upregulated (86) and downregulated (51) human miRNAs assayed in following comparison with the control samples (the average expression signal of the control sample was set as baseline). B and D. Boxplot graphs of expression signals of the human miRNAs with either up or downregulated expression between each experimental tissue type in comparison to control. For each tissue, the average of 4 replicates was taken and log2 transformed.
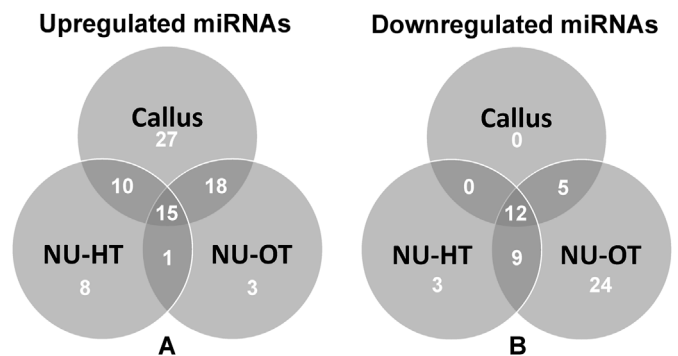
Table 2
Top 20 highest expressed upregulated miRNAs.

Top miRNAs with highest expression in Callus	log2 fold change	Top miRNAs with highest expression in NU-HT	log2 fold change	Top miRNAs with highest expression in NU-OT	log2 fold change
hsa-miR-3197	4.24	hsa-miR-127	4.77	hsa-miR-127	4.83
hsa-miR-127	4.19	hsa-miR-409-3p	4.64	hsa-miR-432	3.77
hsa-miR-4484	4.12	hsa-miR-382	3.82	hsa-miR-409-3p	3.67
hsa-miR-134	4.02	hsa-miR-134	3.72	hsa-miR-199a	3.59
hsa-miR-409-3p	3.71	hsa-miR-199a	3.63	hsa-miR-4253	3.55
hsa-miR-4253	3.63	hsa-miR-432	3.53	hsa-miR-134	3.52
hsa-miR-3663-3p	3.35	hsa-miR-379	3.48	hsa-miR-214	3.37
hsa-miR-199a	3.29	hsa-miR-21	3.48	hsa-miR-3663-3p	3.18
hsa-miR-4532	3.12	hsa-miR-31	3.30	hsa-miR-6840-3p	3.11
hsa-miR-1909	3.02	hsa-miR-132	2.95	hsa-miR-4484	2.96
hsa-miR-150	3.00	hsa-miR-214	2.94	hsa-miR-939	2.93
hsa-miR-6126	2.94	hsa-miR-214	2.74	hsa-miR-6716-5p	2.84
hsa-miR-6824-5p	2.91	hsa-miR-4269	2.67	hsa-miR-4322	2.80
hsa-miR-4486	2.90	hsa-miR-34a	2.61	hsa-miR-574	2.79
hsa-miR-939	2.85	hsa-miR-497	2.55	hsa-miR-1909	2.63
hsa-miR-3178	2.83	hsa-miR-574	2.53	hsa-miR-6782-5p	2.59
hsa-miR-6840-3p	2.83	hsa-miR-99b	2.49	hsa-miR-6784-5p	2.52
hsa-miR-6716-5p	2.82	hsa-miR-654-3p	2.47	hsa-miR-6790-5p	2.51
hsa-miR-432	2.81	hsa-let-7e	2.37	hsa-miR-99b	2.50
hsa-miR-382	2.77	hsa-miR-3187	2.35	hsa-miR-382	2.48
Same in all 3 samples		Same between Callus and NU-OT		Same between NU-HT and NU-OT	

upregulated in the fracture callus and downregulated only in NU-HT and 7 that were upregulated in the fracture callus and downregulated only in NU-OT (Table 4). Conversely, we only found 1 miRNA that was downregulated in the fracture callus but upregulated in NU-HT and 4 that were downregulated in the callus and upregulated in NU-OT. We did not find any miRNAs that were downregulated >0.5 log2 change and upregulated in both nonunion samples (Table 4).

We further examined the miRNAs that were upregulated (>0.5 log2 change) in NU-HT but downregulated in the other two samples by > 0.5 log2 change. We identified one miRNA while no miRNAs were upregulated in NU-HT but downregulated in fracture callus (Table 5). Further, we found two miRNAs that were upregulated in NU-HT but downregulated in NU-OT (Table 5). In addition, we identified one miRNA that was downregulated (>0.5 log2 change) in NU-HT but upregulated in the other two samples by > 0.5 log2 change (Table 5). Further, we found 20 miRNAs that were downregulated in NU-HT but upregulated in the fracture callus (Table 5). Lastly, four miRNAs were downregulated in NU-HT but upregulated in the NU-OT (Table 5).

Lastly, we examined the miRNAs that were upregulated (>0.5 log2 change) in NU-OT but downregulated in the other two samples by > 0.5 fold. We identified one miRNA while three miRNAs were upregulated in NU-OT but downregulated in fracture callus (Table 6). Further, we found five miRNAs that were upregulated in NU-OT but downregulated in NU-HT (Table 6). In addition, no miRNAs were downregulated (>0.5 log2 change) in NU-OT but upregulated in the other two samples by > 0.5 log2 change, while nine miRNAs that were downregulated in NU-OT but upregulated in the fracture callus (Table 6). Lastly, three miRNAs were downregulated in NU-OT but upregulated in the NU-HT (Table 6).

3.3. Bioinformatic biological significance and identification of predicted target genes

To explore the biological significance of the miRNA differential expression in these samples, we first identified the predicted target genes of the expressed miRNAs for each tissues sample (Callus, NU-HT, NU-OT) using miRDB and then conducted gene ontology and pathway enrichment analysis on the target genes using DAVID Bioinformatics Resources. The results of these analyses are shown in Supplementary Tables 8-10 for callus, NU-HT and NU-OT, respectively.

Our enrichment analyses of miRNAs target genes from callus, NU-HT and NU-OT revealed 98, 112 and 137 biological processes, respectively (Supplementary Tables 8 and 10). Many of these processes were representative of key signal transduction pathways, various regulatory processes, developmental processes, etc (Supplementary Tables 8–10). In addition, we also investigated the predicted target genes of miRNAs for each tissue type; callus, NU-HT and NU-OT using gene ontology and pathway enrichment analysis of the target genes. Fig. 5 shows the results of these analyses and it reveals common significant biological processes between the three tissue types as well as similarities between two of the samples, callus and NU-HT (signal transduction and axon guidance) (Fig. 5AB). Further, there are some biological processes that are significantly unique to each sample type; i.e. homophilic cell adhesion via plasma membrane adhesion molecules for the callus sample; memory for NU-HT and negative regulation of transcription, intracellular signal transduction an peptidyl-serine phosphorylation for NU-OT (Fig. 5A–C).

Lastly, KEGG analysis also revealed common gene targets between the three experimental samples involved in specific signaling pathways such as PI3K-Akt, FoxO and MAPK (Fig. 6A–C). On the other hand, there were

Table 3

Top 20 highest expressed downregulated miRNAs.

Top miRNAs with lowest expression in Callus	log2 fold change	Top miRNAs with lowest expression in NU-HT	log2 fold change	Top miRNAs with lowest expression in NU-OT	log2 fold change
hsa-miR-133a	-2.90	hsa-miR-4668-5p	-4.02	hsa-miR-133	-4.71
hsa-miR-133b	-2.82	hsa-miR-3613-3p	-3.91	hsa-miR-133b	-4.62
hsa-miR-1	-2.80	hsa-miR-1	-3.51	hsa-miR-18	-4.39
hsa-miR-378d	-2.71	hsa-miR-150	-3.40	hsa-miR-378f	-4.14
hsa-miR-30e-3p	-2.70	hsa-miR-133a	-3.25	hsa-miR-1	-4.13
hsa-miR-378	-2.50	hsa-miR-378d	-3.13	hsa-miR-378d	-4.11
hsa-miR-378i	-2.46	hsa-miR-206	-2.98	hsa-miR-182	-3.86
hsa-miR-182	-2.41	hsa-miR-1973	-2.97	hsa-miR-128	-3.76
hsa-miR-18	-2.29	hsa-miR-133b	-2.77	hsa-miR-3613-3p	-3.76
hsa-miR-206	-2.27	hsa-miR-182	-2.65	hsa-miR-4668-5p	-3.68
hsa-miR-628	-2.26	hsa-miR-30e-3p	-2.61	hsa-miR-194	-3.67
hsa-miR-128a	-2.24	hsa-miR-18	-2.48	hsa-miR-378i	-3.56
hsa-miR-20	-2.22	hsa-miR-378	-2.43	hsa-miR-20b	-3.49
hsa-miR-20b	-2.12	hsa-miR-363	-2.28	hsa-miR-378c	-3.14
hsa-miR-378c	-2.10	hsa-miR-20b	-2.17	hsa-miR-20	-3.12
hsa-miR-378f	-2.01	hsa-miR-1285	-2.12	hsa-miR-30e-3p	-3.11
hsa-miR-194	-1.97	hsa-miR-378g	-2.10	hsa-miR-422a	-3.08
hsa-miR-378g	-1.94	hsa-miR-378i	-2.10	hsa-miR-378g	-3.01
hsa-miR-29c	-1.84	hsa-miR-4306	-2.09	hsa-miR-378	-2.91

Same in all 3 samples		**Same between Callus and NU-OT**		**Same between NU-H and NH-OT**	
		Same between Callus and NU-HT			

Table 4

Differentially expressed miRNAs.

Upregulated (>0.5 log2 change) miRNAs in Callus but downregulated (>0.5 log2 change) in both NUs	Upregulated (>0.5 log2 change) miRNAs in Callus but downregulated (>0.5 log2 change) in NU-HT	Upregulated (>0.5 log2 change) miRNAs in Callus but downregulated (>0.5 log2 change) in NU-OT
hsa-miR-4440 hsa-miR-3911 hsa-miR-185–3p	hsa-miR-936; hsa-miR-6124; hsa-miR-7152–3p hsa-miR-3917; hsa-miR-4669; hsa-miR-4257 hsa-miR-6831–5p; hsa-miR-3175; hsa-miR-7846–3p hsa-miR-1273 d; hsa-miR-4271; hsa-miR-3131 hsa-miR-5093; hsa-miR-6847–5p; hsa-miR-4800–5p hsa-miR-3907; hsa-miR-765; hsa-miR-6165	hsa-miR-146 b hsa-miR-4284 hsa-miR-4701–3p hsa-miR-7975 hsa-miR-339–5p hsa-miR-224–5p hsa-miR-8073
Downregulated (>0.5 log2 change) miRNAs in Callus but upregulated (>0.5 log2 change) in both NUs	**Downregulated (>0.5 log2 change) miRNAs in Callus but upregulated (>0.5 log2 change) in NU-HT**	**Downregulated (>0.5 log2 change) miRNAs in Callus but upregulated (>0.5 log2 change) in NU-OT**
	hsa-miR-26b-5p	hsa-miR-3613–5p; hsa-miR-4743–5p hsa-mir-6722; hsa-miR-668–5p

other pathways that were significant in both nonunion samples but not in callus. An example of this is a signaling pathway that plays a role in regulating stem cell pluripotency (Fig. 6D). In each schematic, the gene indicated by a red star represents a miRNA target gene identified in our analyses.

4. Discussion

This study represents the first comprehensive approach to decipher the miRNAome of human skeletal tissues such as control bone, fracture callus and two nonunion tissue types (hypertrophic and oligotrophic). Herein we show the differential expression of hundreds of miRNAs (from many species) between control intact bone in comparison to fracture callus and nonunion tissues. But when we examined only the human miRNAs, those numbers decreased to 86 being upregulated and 51 downregulated. Other studies have also reported on miRNA expression during fracture repair in animal models [10,22–24] and many others have reported on individual miRNAs in both animal and human studies [8,9]. Moreover, several studies have also reported on the miRNA profiling in human fractured bones. For example, Dai et al. (2021) [25] described the differential expression of miRNAs isolated from infected human tibial nonunions vs. those from patients with a closed fracture of the tibia. They found 20 significantly differentially expressed miRNAs, 2 upregulated and 18 downregulated. Comparing these data, to our data,

Table 5
Differentially expressed miRNAs.

Upregulated (>0.5 log2 change) miRNAs in NU-HT but downregulated (>0.5 log2 change) in both Callus and NU-OT	Upregulated (>0.5 log2 change) miRNAs in NU-HT but downregulated (>0.5 log2 change) in Callus	Upregulated (>0.5 log2 change) miRNAs in NU-HT but downregulated (>0.5 log2 change) in NU-OT
hsa-miR-26b-5p		hsa-miR-140; hsa-miR-196b-5p
Downregulated (>0.5 log2 change) miRNAs in NU-HT but upregulated (>0.5 log2 change) in both Callus and NU-OT	**Downregulated (>0.5 log2 change) miRNAs in NU-HT but upregulated (>0.5 log2 change) in Callus**	**Downregulated (>0.5 log2 change) miRNAs in NU-HT but upregulated (>0.5 log2 change) in NU-OT**
hsa-miR-4271	hsa-miR-6165; hsa-miR-1273d; hsa-miR-936 hsa-miR-4669; hsa-miR-3911; hsa-miR-185–3p hsa-miR-5093; hsa-miR-4440; hsa-miR-6831–5p hsa-miR-6124; hsa-miR-3175; hsa-miR-3131 hsa-miR-7846–3p; hsa-miR-6847–5p; hsa-miR-7152–3p hsa-miR-4257; hsa-miR-4800–5p; hsa-miR-3917 hsa-miR-765; hsa-miR-3907	hsa-miR-4487 hsa-miR-1273f hsa-miR-668–5p hsa-miR-371 b-5p

Table 6
Differentially expressed miRNAs. (Please note that there is space between the top part and bottom part of the Table - please join as you did for Table 4 and 5 and the highlighted rown should have a grey background.

| Upregulated (>0.5 log2 change) miRNAs in NU-OT but downregulated (>0.5 log2 change) in both Callus and NU-HT	Upregulated (>0.5 log2 change) miRNAs in NU-OT but downregulated (>0.5 log2 change) in Callus	Upregulated (>0.5 log2 change) miRNAs in NU-OT but downregulated (>0.5 log2 change) in NU-HT
hsa-miR-668–5p	hsa-miR-3613–5p; hsa-mir-6722 hsa-miR-4743–5p	hsa-miR-1273f; hsa-miR-4487; hsa-miR-371 b-5p hsa-miR-4271; hsa-miR-877–5p
Downregulated (>0.5 log2 change) miRNAs in NU-OT but upregulated (>0.5 log2 change) in both Callus and NU-HT	**Downregulated (>0.5 log2 change miRNAs in NU-OT but upregulated (>0.5 log2 change) in Callus**	**Downregulated (>0.5 log2 change) miRNAs in NU-OT but upregulated (>0.5 log2 change) in NU-HT**
	hsa-miR-4284; hsa-miR-7975; hsa-miR-4440 hsa-miR-339–5p; hsa-miR-3911; hsa-miR-224–5p hsa-miR-185–5p; hsa-miR-8073; hsa-miR-146b-5p	hsa-miR-26b-5p hsa-miR-140–5p hsa-miR-196b-5p
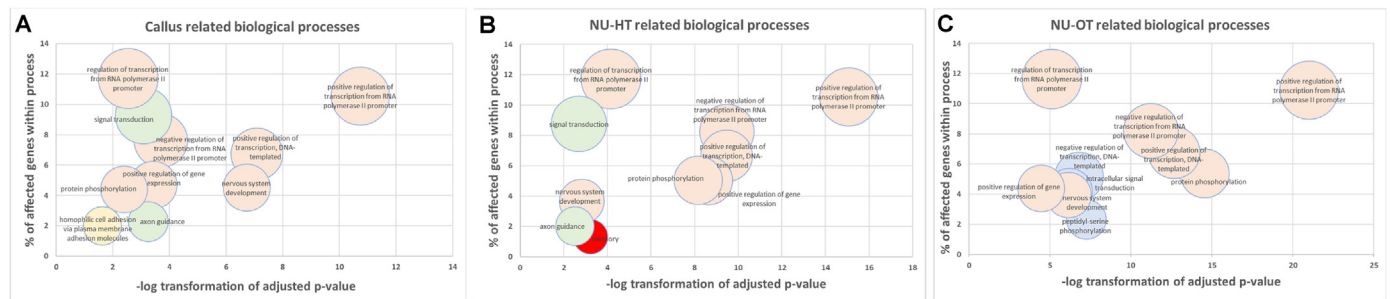
Fig. 5. Biological process analyses. Plots showing biological processes affected by miRNAs expressed in Callus (A), NU-HT (B) and NU-OT (C). Salmon color indicates similar processes between the three samples, whereas green is between Callus and NU-HT. Yellow, blue and red indicate significant biological processes only present with target genes of miRNAs expressed in those individual samples.

we did not find any common miRNAs either up or down-regulated, probably as a result of differences in the samples used; in our study there were no infected samples.

In a more relevant study examining miRNA between bony callus and atrophic nonunion, Chen et al. (2019) [26], identified only 4 and 7 miRNAs that were up and down-regulated, respectively. Examination of the expression of these 11 differentially expressed miRNAs did not appear as such in our data set, again probably because our samples were not atrophic; they were hypertrophic and oligotrophic. Similarly, Wei et al. (2020) [27], also investigated global miRNA expression between a fracture healed group and atrophic nonunion and identified 113 miRNAs, with only 9 that were upregulated in nonunion with a >1.5 fold and another 9 that were downregulated with a <0.67 fold. Once again, we did not detect any of these differentially expressed miRNAs in our samples, including both nonunion samples. Lastly, Groven et al. (2022) [28] examined various stages of human physiological fracture healing utilizing inflammatory and fibrosis arrays and identified 43 and 56 differentially expressed miRNAs, respectively. Some of the identified differentially expressed miRNAs were also consistent with our data; i.e. miR-21–5p, that was upregulated in their fibrotic and inflammatory array was also upregulated in our samples. Similarly, we also identified 6

downregulated miRNAs (miR-491–5p; miR-335–5p; miR-10a-5p; miR-146a-5p; miR-122a-3p; miR-192–5p) in our samples that were also downregulated in their fibrotic array data. Lastly, two miRNAs, miR-520a and miR200a-3p in our samples were also consistently downregulated as was the case with their inflammatory array.

Our data set revealed that from the top 20 upregulated miRNAs, 6 (miR-127, miR-409–3p, miR-382, miR-134, miR-199a, and miR-432) are found in the three experimental samples (fracture callus, NU-HT and NU-OT) and indicates that there are molecular similarities between these samples which is not surprising since we find similar tissues/cell types in the fracture callus and nonunions histologically. Further, five of these six miRNAs are associated with the skeletal system. For example, miR-127 was previously shown to be upregulated in bone following ovariectomy and its inhibition stimulated osteoblastic differentiation [29]. miR-409–3p was also found to promote osteoblastic differentiation via activation of Wnt/β-catenin signaling pathway [30]. Similarly, miR-382 was also found to be involved in adipogenic and osteogenic differentiation of bone mesenchymal stem cells [31]. In contrast, miR-134 was shown to inhibit chondrogenic differentiation of bone marrow mesenchymal stem cells by targeting SMAD6 [32]. Finally, it was previously demonstrated that miR-199a counteracts glucocorticoid inhibition of
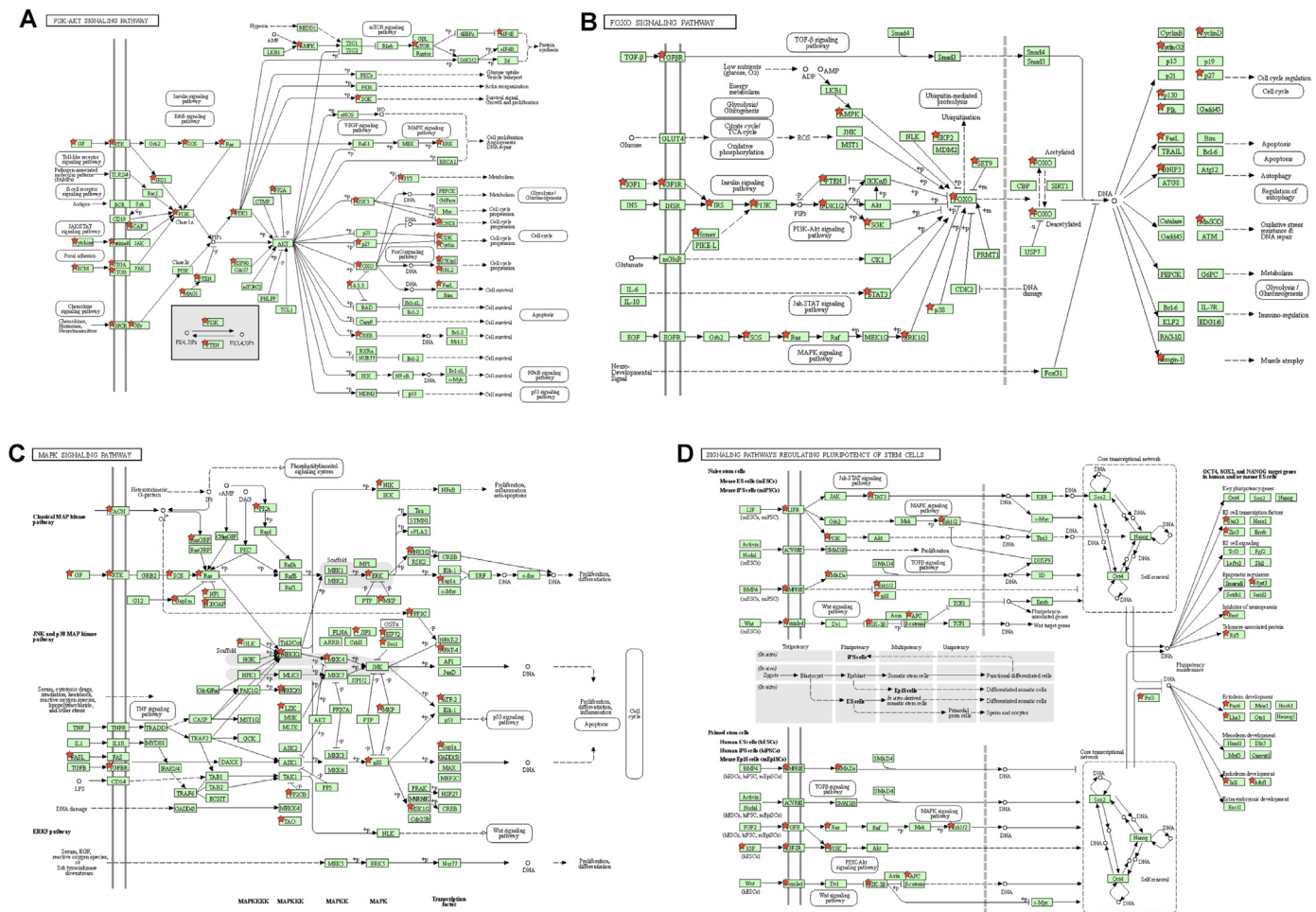
Fig. 6. Biological process analyses. Signaling pathways shown in A-C are all affected by miRNAs expressed in Callus, NU-HT and NU-OT. Signaling pathway shown in D is only affected by miRNAs expressed by the both nonunions samples only. Genes denoted by a red star indicate miRNA target genes identified in our analyses.

bone marrow mesenchymal stem cell osteogenic differentiation through regulation of Klotho [33].

We also found 11 common downregulated miRNAs from the top 20 (miR-133a, miR-133b, miR-1, miR-378d, miR-30e-3p, miR-378, miR-378i, miR-182, miR-18, miR-20b, miR-378g). What is more importantly is that we were able to identify 3 miRNAs (miR-4440, miR-3911, miR-185–3p) that were specifically upregulated in the fracture callus but downregulated in both nonunion tissues. In examining the literature, we found that miR-4440 is associated with various cancers [34–36] and in one of these studies it was shown that its over-expression may enhance proliferation, invasion and migration of breast cancer cells [34]. Previously, it was reported that miR-3911 was upregulated in diabetic nephropathy [37] and downregulated in the blood of patients with autosomal dominant polycystic kidney disease [38]. Lastly, miR-3911 was also detected in patients with Amyotrophic Lateral Sclerosis (ALS) [39] and upregulated in response to treatment of human early endothelial progenitor cells with brain-derived neurotrophic factor (BDNF) [40]. Although there is a large number of manuscripts describing the expression and perturbation of miR-185–3p, the majority of them involve cancer cells and several indicate that miR-185–3p plays a role in promoting tumor growth by mediating RAB25 [41] and targeting Annexin-A8 to inhibit proliferation in cervical cancer cells [42]. Collectively then, nothing is known about the expression or role of these three miRNAs in the skeletal system. The fact that they are upregulated in the fracture callus and downregulated in the nonunion tissues makes them potential candidate miRNAs for further study, as they may turn out to be critical in normal physiological fracture repair.

Unfortunately, we did not find any miRNAs that were downregulated in the callus but upregulated in both nonunion tissues. Instead, we found one (miR-26b-5p) and four (miR-3613–5p, miR-4743–5p, miR-6722, miR-668–5p) miRNAs that were downregulated in the facture callus and upregulated in NU-HT and NU-OT, respectively. Interestingly, miR-26b-5p was previously found to inhibit liver fibrogenesis and angiogenesis by targeting PDGFR-β [43]. It was also demonstrated that miR-26b-5p serves as a negative regulator of proliferation, angiogenesis, and apoptosis in hepatocellular carcinoma [44]. As such, further exploration of miR-26b-5p′s role in angiogenesis during fracture repair is warranted. miR-3613–5p was also shown to be associated with cancer cell proliferation [45]. No other relevant information was reported in the literature for miR-4743–5p, miR-6722 and miR-668–5p.

We also discovered that differential expression of miRNAs between the two nonunion samples. For example, miR-140 and miR-196b-5p were upregulated in NU-HT but downregulated in NU-OT. Interestingly, miR-140 was previously shown to be upregulated in a mouse nonunion model (femoral osteotomy model in CD-1 mice) concomitant with a decreased expression of SDF-1α and Dnpep, both known to be miR-140 target proteins [46]. It was previously showed that these two proteins have key roles in fracture repair [47,48] and that SDF-1α is required for the biological effect of BMP-2 [49,50] which of course it is a potent osteogenic factor and promotes bone repair [51]. Lastly, the authors suggested that the development of a nonunion may be due to an indirect inhibitory effect on BMP-2 through the downregulation of SDF-1α by miR-140 [46].

In contrast, miR-4487, miR-1273f, miR-668–5p and miR-371b-5p were found to be downregulated in NU-HT but upregulated in NU-OT.

The first three miRNAs were previously found to be associated with various cancers and thus nothing is known about their function in the skeletal system. And although miR-371b-5p is also associated with various cancers, it was previously identified as a monocyte-related biomarker of rheumatoid arthritis development [52] as well as expressed in chondrosarcoma [53]. Lastly, it was also reported that alveolar progenitor type II cell-derived exosome miR-371b-5p may serve as a niche signaling to augment ATIIC survival/proliferation (via targeting PTEN, which stimulates phosphorylation of Akt and its downstream substrates, GSK3β and FOXOs) and promotes re-epithelialization of injured alveoli [54]. As this data suggest a role for miR-371 b-5p during injury, it is conceivable then that it may have the same function in cells of the fracture callus, especially during oligotrophic nonunion development.

Our data also revealed many potential target genes for the differentially expressed miRNAs. Of course, these are all predictive target genes and some of them are related to the skeletal system, such as BMP-6 (target of miR-150–3p), BMP-3 (target of miR-34a-5p and miR-19b-3p), BMP receptor type 1 (target of miR-182–5p) and type 2 (target of miR-494–3p, miR-20a-5p, miR-363–3p, miR-106b-5p), osteoglycin (target of miR-379–5p and miR-494–3p), osteoclastogenesis associated transmembrane protein 1 (target of miR-20b-5p), osteonectin (target of miR-19b-3p) and TGF-β (target of miR-21–5p). Clearly, all of these as well as other relevant target mRNAs will need to be experimentally verified.

Our final bioinformatic enrichment analysis of target genes of miRNAs from each experimental sample revealed the existence of common biological processes between them; transcriptional regulation, protein phosphorylation, and nervous system development. In addition, there were a couple of biological processes (signal transduction and axon guidance) that were affected by miRNAs expressed in the fracture callus and NU-HT but not in the NU-OT. This indicates that a hypertrophic nonunion is more similar to fracture callus as both develop a callus whereas no callus is present in an oligotrophic nonunion. Further, target genes of miRNAs expressed in the three experimental samples implicate various signaling pathways, predominantly, PI3K-Akt, FoxO and MAPK, all known to play a role in fracture repair [8]. Our miRNA target gene analyses also revealed one pathway regulating the pluripotency of stem cells, but this was only significantly present in the two nonunions but not in the fracture callus. Clearly, this may represent an important finding as it indicates that perhaps disruptions in stem cell differentiation pathways by miRNAs may result in nonunions. Obviously, these data need to be experimentally verified in order to be able to positively proof that this may indeed be the cause of nonunions.

Finally, we have identified a few limitations associated with our study. For example, our control bones were all obtained from the ileac crest which is a flat bone whereas our experimental bones were all derived from various long bones and thus there may be some inherent molecular differences. In addition, we did not have the same age or gender within each group and between groups. Lastly, the timing of the callus varied between samples as well. As such, there is variability in tissue from patient to patient within each group and between groups. Unfortunately, this is the reality as sampling from humans is not easy; there is no perfect sampling time or patient characteristics. Also, the experimental design of this study did not allow a temporal analysis of individual miRNA expression which could have linked specific miRNAs with the individual processes (inflammation, angiogenesis, osteogenesis, chondrogenesis, ossification, etc.) that occur during fracture repair. But it did identify hundreds of differentially expressed miRNAs in fracture calluses as well as in both, hypertrophic and oligotrophic nonunion tissues. Many of these miRNAs are from other species (non-human) and thus they will need to be further examined, especially by those that work on rodents. As these were human samples, we focused on the human miRNAs but by no means they are the only important ones. And this is the main reason why we chose to include the nonhuman data, so that other scientists working on other species can have access to the data as it

pertains to their animal model. Having this data will enable us to conduct downstream studies to decipher the function of some of these regulatory RNAs, especially in the skeletal system and more importantly, during physiological and aberrant fracture repair.

And perhaps in the future some of these miRNAs identified in this study, once deciphered in greater detail, they can be used as miRNA-based orthobiologics, especially as several miRNA-based therapeutics have recently entered clinical trials for non-skeletal applications as well as for diagnostic markers in skeletal conditions such as osteoporosis, bone metastases and hypophosphatasia.

(*B*) *AP radiograph of a left tibia and fibula nonunion in 62-year healthy old male. Initial fracture treatment was done 2 years prior. The nonunion was classified as a hypertrophic nonunion (NU-HT, according Weber and Cech) because of the elephant foot appearance. Tissue was obtained from the center of the nonunion as indicated by the arrow (C) AP radiograph of left tibia shaft and fibula nonunion in a 47-year old healthy female. The nonunion was classified as an oligotrophic nonunion (NU-OT, according to Weber and Cech). A small portion of nonunion tissue was obtained from the central part as indicated by arrow. This paragraph is part of Fig. 1 legend.*

Author contributions

MH: conceptualization; methodology; validation; investigation; data curation; writing; visualization; supervision; project administration; funding acquisition. LS: formal analysis; investigation; data curation. PK: conceptualization; methodology; investigation; resources; writing; visualization; supervision; project administration.

Declaration of competing interest

The authors declare that they have no conflicts of interest with the contents of this article.

Acknowledgements

Appendix A. Supplementary data

Supplementary data to this article can be found online at https://doi.org/10.1016/j.jot.2023.01.005.

References

[1] Hadjiargyrou M, O'Keefe RJ. The convergence of fracture repair and stem cells: interplay of genes, aging, environmental factors and disease. J Bone Miner Res 2014 Nov;29(11):2307–22.

[2] Weber BG, Pseudarthrosis Cech O. Pathophysiology, biomechanics, therapy, results. New York, NY, USA: Grune & Stratton; 1976.

[3] Elliott DS, Newman KJ, Forward DP, Hahn DM, Ollivere B, Kojima K, et al. A unified theory of bone healing and nonunion: BHN theory. Bone Joint Lett J 2016 Jul;98-B(7):884–91.

[4] Brownlow HC, Reed A, Simpson AH. The vascularity of atrophic non-unions. Injury 2002 Mar;33(2):145–50.

[5] Sampath TK, Reddi AH. Discovery of bone morphogenetic proteins - a historical perspective. Bone 2020 Nov;140:115548.

[6] Wojda SJ, Donahue SW. Parathyroid hormone for bone regeneration. J Orthop Res 2018 Oct;36(10):2586–94.

[7] Cheng C, Shoback D. Mechanisms underlying normal fracture healing and risk factors for delayed healing. Curr Osteoporos Rep 2019 Feb;17(1):36–47.

[8] Komatsu DE, Duque E, Hadjiargyrou M. MicroRNAs and fracture healing: pre-clinical studies. Bone 2021 Feb;143:115758.

[9] Hadjiargyrou M, Komatsu DE. The therapeutic potential of MicroRNAs as orthobiologics for skeletal fractures. J Bone Miner Res 2019 May;34(5):797–809.

[10] Hadjiargyrou M, Zhi J, Komatsu DE. Identification of the microRNA transcriptome during the early phases of mammalian fracture repair. Bone 2016 Jun;87:78–88.

[11] Hadjiargyrou M, Ahrens W, Rubin CT. Temporal expression of the chondrogenic and angiogenic growth factor CYR61 during fracture repair. J Bone Miner Res 2000 Jun;15(6):1014–23.

[12] Zhi J, Sommerfeldt DW, Rubin CT, Hadjiargyrou M. Differential expression of neuroleukin in osseous tissues and its involvement in mineralization during osteoblast differentiation. J Bone Miner Res 2001 Nov;16(11):1994–2004.

[13] Lombardo F, Komatsu D, Hadjiargyrou M. Molecular cloning and characterization of Mustang, a novel nuclear protein expressed during skeletal development and regeneration. Faseb J 2004 Jan;18(1):52–61.

[14] Komatsu DE, Hadjiargyrou M. Activation of the transcription factor HIF-1 and its target genes, VEGF, HO-1, iNOS, during fracture repair. Bone 2004 Apr;34(4):680–8.

[15] Gersch RP, Lombardo F, McGovern SC, Hadjiargyrou M. Reactivation of Hox gene expression during bone regeneration. J Orthop Res 2005 Jul;23(4):882–90.

[16] Komatsu DE, Bosch-Marce M, Semenza GL, Hadjiargyrou M. Enhanced bone regeneration associated with decreased apoptosis in mice with partial HIF-1alpha deficiency. J Bone Miner Res 2007 Mar;22(3):366–74.

[17] Abdelmagid SM, Barbe MF, Hadjiargyrou M, Owen TA, Razmpour R, Rehman S, et al. Temporal and spatial expression of osteoactivin during fracture repair. J Cell Biochem 2010 Oct 1;111(2):295–309.

[18] Therneau T, Atkinson B. rpart: Recursive Partitioning and Regression Trees. R package version 2019;4:1–15. https://CRAN.R-project.org/package=rpart.

[19] Griffiths-Jones S, Grocock RJ, van Dongen S, Bateman A, Enright AJ. miRBase: microRNA sequences, targets and gene nomenclature. Nucleic Acids Res 2006;34(Database issue):D140–4.

[20] Wang X. miRDB: a microRNA target prediction and functional annotation database with a wiki interface. RNA 2008;14(6):1012–7.

[21] Huang DW, Sherman BT, Tan Q, et al. DAVID Bioinformatics Resources: expanded annotation database and novel algorithms to better extract biology from large gene lists. Nucleic Acids Res 2007;35:W169–75. Web Server issue).

[22] Li X, Zhong Z, Ma E, Wu X. Identification of miRNA regulatory networks and candidate markers for fracture healing in mice. Comput Math Methods Med 2021;2021:2866475.

[23] Takahara S, Lee SY, Iwakura T, Oe K, Fukui T, Okumachi E, et al. Altered microRNA profile during fracture healing in rats with diabetes. J Orthop Surg Res 2020 Apr 7;15(1):135.

[24] Waki T, Lee SY, Niikura T, Iwakura T, Dogaki Y, Okumachi E, et al. Profiling microRNA expression during fracture healing. BMC Muscoskel Disord 2016 Feb 16;17:83.

[25] Dai Y, Huang L, Zhang H, Hong G, He Y, Hu J, et al. Differentially expressed microRNAs as diagnostic biomarkers for infected tibial nonunion. Injury 2021 Jan;52(1):11–8.

[26] Chen H, Ji X, She F, Gao Y, Tang P. miR-628-3p regulates osteoblast differentiation by targeting RUNX2: possible role in atrophic nonunion. Int J Mol Med 2017 Feb;39(2):279–86.

[27] Wei J, Chen H, Fu Y, Zhang B, Zhang L, Tao S, et al. Experimental study of expression profile and specific role of human microRNAs in regulating atrophic bone nonunion. Medicine (Baltim) 2020 Sep 4;99(36):e21653.

[28] Groven RVM, Peniche Silva CJ, Balmayor ER, van der Horst BNJ, Poeze M, Blokhuis TJ, et al. Specific microRNAs are associated with fracture healing phases, patient age and multi-trauma. J Orthop Translat 2022 Aug 31;37:1–11.

[29] An JH, Ohn JH, Song JA, Yang JY, Park H, Choi HJ, et al. Changes of microRNA profile and microRNA-mRNA regulatory network in bones of ovariectomized mice. J Bone Miner Res 2014 Mar;29(3):644–56.

[30] Chen N, Yang H, Song L, Li H, Liu Y, Wu D. MicroRNA-409-3p promotes osteoblastic differentiation via activation of Wnt/β-catenin signaling pathway by targeting SCAI. Biosci Rep 2021 Jan 29;41(1):BSR20201902.

[31] Xu X, Jiang H, Li X, Wu P, Liu J, Wang T, et al. Bioinformatics analysis on the differentiation of bone mesenchymal stem cells into osteoblasts and adipocytes. Mol Med Rep 2017 Apr;15(4):1571–6.

[32] Xu S, Wu X. miR-134 inhibits chondrogenic differentiation of bone marrow mesenchymal stem cells by targetting SMAD6. Biosci Rep 2019 Jan 30;39(1):BSR20180921.

[33] Tang J, Yu H, Wang Y, Duan G, Wang B, Li W, et al. microRNA-199a counteracts glucocorticoid inhibition of bone marrow mesenchymal stem cell osteogenic differentiation through regulation of Klotho expression in vitro. Cell Biol Int 2020 Dec;44(12):2532–40.

[34] Sun Q, Chong F, Jiang X, Wang Y, Xu K, Zou Y, et al. Association study of SNPs in LncRNA CDKN2B-AS1 with breast cancer susceptibility in Chinese Han population. Int J Biochem Cell Biol 2022 Feb;143:106139.

[35] Alfardus H, de Los Angeles Estevez-Cebrero M, Rowlinson J, Aboalmaaly A, Lourdusamy A, Abdelrazig S, et al. Intratumour heterogeneity in microRNAs expression regulates glioblastoma metabolism. Sci Rep 2021 Aug 5;11(1):15908.

[36] Sayagués JM, Corchete LA, Gutiérrez ML, Sarasquete ME, Del Mar Abad M, Bengoechea O, et al. Genomic characterization of liver metastases from colorectal cancer patients. Oncotarget 2016 Nov 8;7(45):72908–22.

[37] Tu C, Wei L, Wang L, Tang Y. Eight differential miRNAs in DN identified by microarray analysis as novel biomarkers. Diabetes Metab Syndr Obes 2022 Mar 24;15:907–20.

[38] Kocyigit I, Taheri S, Sener EF, Eroglu E, Ozturk F, Unal A, et al. Serum micro-rna profiles in patients with autosomal dominant polycystic kidney disease according to hypertension and renal function. BMC Nephrol 2017 May 30;18(1):179.

[39] Panio A, Cava C, D'Antona S, Bertoli G, Porro D. Diagnostic circulating miRNAs in sporadic amyotrophic lateral Sclerosis. Front Med 2022 May 6;9:861960.

[40] He T, Sun R, Li Y, Katusic ZS. Effects of brain-derived neurotrophic factor on MicroRNA expression profile in human endothelial progenitor cells. Cell Transplant 2018 Jun;27(6):1005–9.

[41] Wang X, Zhu X, Zhao Y. Targeting miR-185-3p inhibits head and neck squamous cell carcinoma by modulating RAB25. Front Oncol 2021 Nov 15;11:721416.

[42] Zhang W, Han D. miR-185-3p targets Annexin-A8 to inhibit proliferation in cervical cancer cells. Cytotechnology 2021 Aug;73(4):585–92.

[43] Yang L, Dong C, Yang J, Yang L, Chang N, Qi C, et al. MicroRNA-26b-5p inhibits mouse liver fibrogenesis and angiogenesis by targeting PDGF receptor-beta. Mol Ther Nucleic Acids 2019 Jun 7;16:206–17.

[44] Wang Y, Sun B, Sun H, Zhao X, Wang X, Zhao N, et al. Regulation of proliferation, angiogenesis and apoptosis in hepatocellular carcinoma by miR-26b-5p. Tumour Biol 2016 Aug;37(8):10965–79.

[45] He T, Shen H, Wang S, Wang Y, He Z, Zhu L, et al. MicroRNA-3613-5p promotes lung adenocarcinoma cell proliferation through a RELA and AKT/MAPK positive feedback loop. Mol Ther Nucleic Acids 2020 Sep 26;22:572–83.

[46] Orth M, Scheuer C, Backes C, Keller A, Rollmann MF, Braun BJ, et al. Profiling microRNA expression in murine bone healing and nonunion formation: role of miR-140 during the early stage of bone healing. PLoS One 2019 Jul 19;14(7):e0218395.

[47] Nicolas FE, Pais H, Schwach F, Lindow M, Kauppinen S, Moulton V, et al. Experimental identification of microRNA-140 targets by silencing and overexpressing miR-140. RNA 2008;14:2513–20.

[48] Nakamura Y, Inloes JB, Katagiri T, Kobayashi T. Chondrocyte-specific microRNA-140 regulates endochondral bone development and targets Dnpep to modulate bone morphogenetic protein signaling. Mol Cell Biol 2011;31:3019–28.

[49] Hosogane N, Huang Z, Rawlins BA, Liu X, Boachie-Adjei O, Boskey AL, et al. Stromal derived factor-1 regulates bone morphogenetic protein 2-induced osteogenic differentiation of primary mesenchymal stem cells. Int J Biochem Cell Biol 2010;42:1132–41.

[50] Hwang HD, Lee JT, Koh JT, Jung HM, Lee HJ, Kwon TG. Sequential treatment with SDF-1 and BMP-2 potentiates bone formation in calvarial defects. Tissue Eng 2015;21:2125–35.

[51] Czech T, Oyewumi MO. Overcoming barriers confronting application of protein therapeutics in bone fracture healing. Drug Deliv Transl Res 2021 Jun;11(3):842–65.

[52] Kurowska W, Kuca-Warnawin E, Radzikowska A, Jakubaszek M, Maślińska M, Kwiatkowska B, et al. Monocyte-related biomarkers of rheumatoid arthritis development in undifferentiated arthritis patients - a pilot study. Reumatologia 2018;56(1):10–6.

[53] Mutlu S, Mutlu H, Kirkbes S, Eroglu S, Kabukcuoglu YS, Kabukcuoglu F, et al. The expression of miR-181a-5p and miR-371b-5p in chondrosarcoma. Eur Rev Med Pharmacol Sci 2015 Jul;19(13):2384–8.

[54] Quan Y, Wang Z, Gong L, Peng X, Richard MA, Zhang J, et al. Exosome miR-371b-5p promotes proliferation of lung alveolar progenitor type II cells by using PTEN to orchestrate the PI3K/Akt signaling. Stem Cell Res Ther 2017 Jun 8;8(1):138.